INCREASED SPATIAL AND TEMPORAL CONSISTENCY OF LEAFY SPURGE MAPS FROM MULTIDATE AVIRIS IMAGERY: A MODIFIED, HYBRID LINEAR SPECTRAL MIXTURE ANALYSIS/MIXTURE-TUNED MATCHED FILTERING APPROACH

Kathleen Burke Dudek,[1] Ralph R. Root,[2] Raymond F. Kokaly,[3] Gerald L. Anderson[4]

1. INTRODUCTION

Imaging spectroscopy has been predominantly used for research-oriented studies, although more recently there has been increased interest in exploiting imaging spectroscopy to address applied problems. Applied work has lagged behind in part due to the complex, interactive processing that hyperspectral imagery requires and to the associated "learning curve." Land managers may be aware of the potential benefits of the technology for ecological monitoring, but are most often not well versed in hyperspectral processing and analysis. Current processing methods require specialized training or advanced experience in remote sensing in order to determine the most appropriate methods to use, to make informed decisions during interactive processing, and to determine whether results are realistic and accurate.

The intent of this work was to develop specific strategies to facilitate and streamline analysis, and eliminate interactive steps that require in-depth knowledge of the ground to guide processing decisions. If the need for advanced training or experience can be minimized, imaging spectroscopy may become a more widespread tool for ecological and other applied work. In the application tested here, the suitability of multi-temporal AVIRIS data for monitoring change in *Euphorbia esula* L. (leafy spurge) over a two-year period was evaluated. High altitude AVIRIS data were collected 6 July 1999 and 21 June 2001 over Theodore Roosevelt National Park (THRO) (Figure 1). A specific goal was to determine which methods are most appropriate for applied work, as well as evaluate problems that are unique to multi-temporal imaging spectroscopy. Successful management of leafy spurge over time, and monitoring of ecosystem characteristics in general, requires reliable identification of plants over time and space. This necessitates processing methods that are explicitly defined and repeatable, and that yield accurate and consistent results. Imaging spectroscopy has been used previously to map invasive species including leafy spurge (DiPietro et al., 2002; Kokaly et al., 2001; O'Neill et al., 2000; Parker-Williams and Hunt, 2002; Root et al., 2002). Relatively few studies, however, have used multi-temporal imaging spectroscopy, and fewer still have focused on problems that are uniquely encountered with multi-temporal hyperspectral data processing. Primary applications of remote sensing in general include monitoring and change detection, yet imaging spectroscopy has been underexploited in these areas.

Leafy spurge is an aggressive perennial invasive that was introduced into the U.S. and Canada in the early 19th century and has since spread throughout much of North America (Anderson et al., 2003; Dunn, 1979, 1985). It is a particularly serious problem in the northern Great Plains States and Prairie Provinces of Canada, where it has serious economic and environmental consequences (Bangsund et al., 1993; Beck, 1996; Leitch et al., 1994; Wallace et al., 1992). It is difficult to monitor due to a relatively non-selective habitat, ranging from dry hills to swampy riparian habitats throughout remote rangelands, wildlands, and cultivated and disturbed areas (Callihan et al., 1990; Galitz, 1994). The weed requires a substantial effort to control, with greatest success realized when small, emergent patches are treated within the first years of establishment (Lajeunesse et al., 1997). Imaging spectroscopy has been suggested as a means for locating smaller, nascent patches that are often fragmented and difficult to locate, as well as for temporal monitoring of treatments that have been applied over larger established infestations.

To streamline, refine, and automate current processing, standard hyperspectral mapping methods were tested and modified within a commercially available software package, Environment for Visualizing

[1] Dept. of Forest, Rangeland, and Watershed Stewardship, Colorado State University (kaydudek@cnr.colostate.edu)
[2] Deceased
[3] USGS Spectroscopy Laboratory
[4] USDA, ARS, Northern Plains Agricultural Research Laboratory

Systems (ENVI). Specific objectives for the refinement included: decreasing the influence of analyst decisions or bias; decreasing the need for expert knowledge or advanced training; decreasing the need for ground support or reference data; and decreasing the need for conclusive *a priori* knowledge of the target endmember spectrum. The ultimate goal of the project is to produce accurate and *consistent* multi-temporal maps and avoid misinterpretations due to apparent change (e.g., changes that are a reflection of differences in processing over time rather than real landcover change).

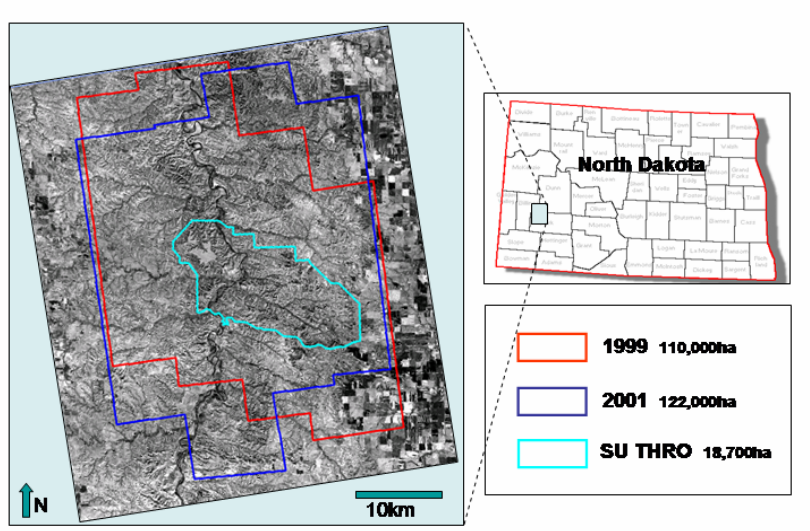

Figure 1. Study area: South Unit THRO and adjacent National Grasslands, South Unit outlined in cyan. AVIRIS coverage indicated in red (1999) and blue (2001), 4 flightlines per date with 35-40% sidelap.

2. PREVIOUS WORK

The potential impact of differences in processing methodology was suggested by initial test maps. These maps of leafy spurge were produced using several different algorithms, including spectral angle mapper (SAM) (Kruse et al., 1993), linear spectral mixture analysis (SMA) (Adams et al., 1993), spectral feature fitting (SFF) (Clark et al., 1990), and mixture-tuned matched filtering (MTMF) (Boardman, 1998). The results indicated that the proportion of leafy spurge that was mapped varied dramatically depending on the algorithm that was used (Figure 2). The map results were also sensitive to threshold decisions as well as some preprocessing steps including band editing, cross-track illumination correction, and image masking. The source and quality of the spectral library also impacted the results (see discussion in Dudek, 2005). The variability of the results produced from identical data that were associated strictly with processing differences suggests that change maps produced from independently-processed, multi-temporal hyperspectral imagery could therefore include spurious results and a misleading representation of change. Apparent change could instead represent an artifact of processing rather than true temporal differences in landcover. This in turn could lead to erroneous interpretation of the effect of controls and the advance and decline of infestations, which could result in inappropriate decisions regarding treatment effects and future management decisions.

3. METHODS

Standard hyperspectral preprocessing and processing methods were applied and have been described previously (Root et al., 2002). These included, for example, calibration to reflectance using ACORN software (Atmospheric Correction Now) and georeferencing using a thin plate spline model (Geomatica User Guide, 2003).

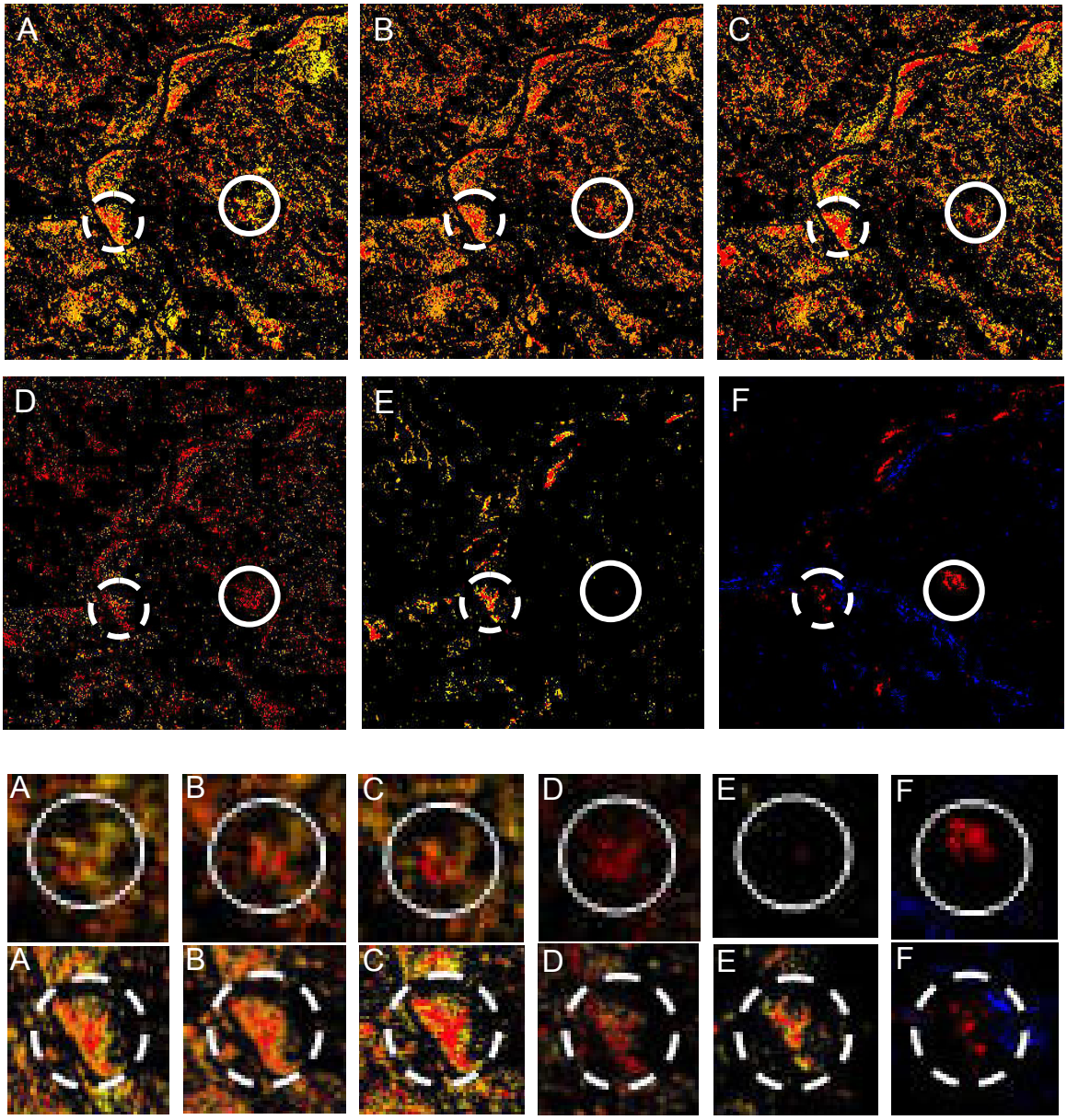

Figure 2. Leafy spurge test maps from identical data. All methods except E incorrectly mapped the assemblage within the solid circles as leafy spurge. The area of known leafy spurge (broken circles) was mapped with all methods but was over-classified in A, B, and C; under-classified in F; and slightly under-classified in E. E is considered most accurate overall and therefore was the method selected as a starting point for the modifications and refinements.

Preprocessing steps that were crucial for accurate mapping included: cross-track illumination correction (ENVI User's Guide, 2003; Kennedy et al., 1997) and liberal editing of bands, including removal of bands displaying anomalous spikes within the chlorophyll absorption region. The MTMF algorithm in conjunction with an image-derived endmember library produced the most accurate results and was therefore selected for all additional processing and refinement (see Figure 2E).

Once preprocessing was completed, the mapping technique generally followed the "hourglass" mapping scheme (CSES, 2000), but with several modifications (Figure 3). These included: 1) a two-step endmember selection: first, for general landcover classes, followed by collection of vegetation

endmembers only from an NDVI-masked image; the collection strategy was modified for the masked image endmember selection; 2) for each additional flightline on a given date (in a scene), a minimum noise fraction (MNF) re-transformation of the spectral library derived from a single flightline; 3) hybrid application of the MTMF algorithm: input all possible endmembers; solve for all endmember fractions; 4) modified application of the MTMF algorithm: eliminate threshold decisions by first using rule classification to assign MF thresholds, then using +1 sigma from the mean noise units as a standard threshold for infeasibility score refinement. These steps are described in detail below.

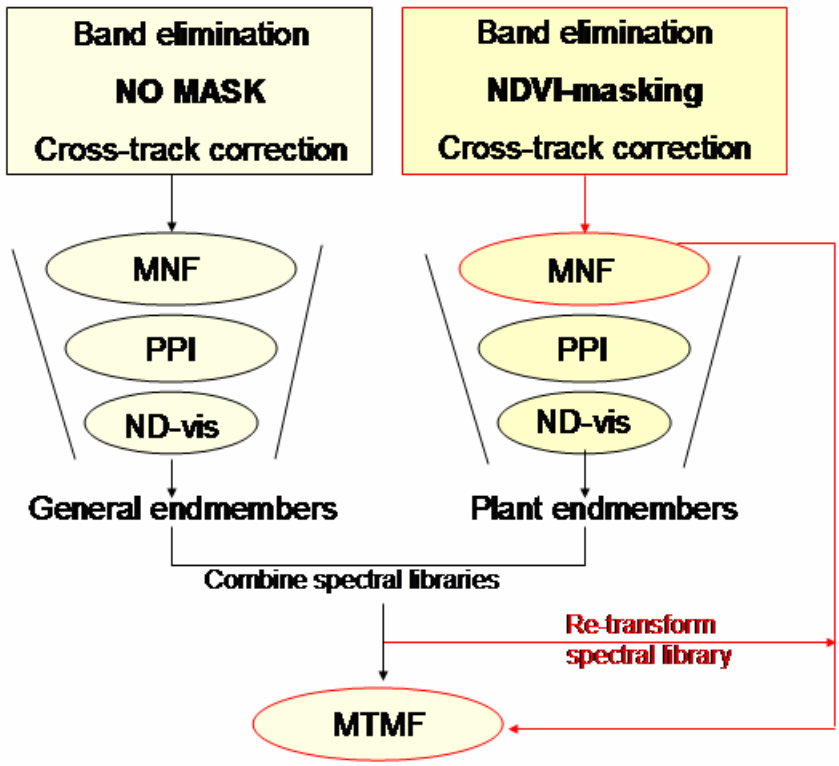

Figure 3. Modified hourglass processing: two-stage endmember collection for the initial flightline, with the added second step indicated in darker yellow; additional steps for subsequent flightlines on each date are outlined in red. Critical preprocessing steps are indicated in the two boxes, listed in the order applied.

3.1 Two-stage endmember library collection

For mapping, two endmember libraries were derived independently from the image. It was necessary to extract a full set of general landcover endmembers from the full image in order to correctly derive endmember fractions in vegetation-dominated pixels containing inert materials as a minor component. Initially, the full non-masked image was transformed with the minimum noise fraction (MNF) to decrease noise and reduce the dimensionality of the data set (Green et al., 1988). With the pixel purity index (PPI), the most spectrally unique individual pixel spectra were isolated and input to the n-dimensional visualizer in ENVI to collect a set of general landcover endmembers (Figure 4A) (ENVI, 2003). Twenty-two input MNF bands were sufficient to represent the variance of, and therefore isolate, these major landcover classes.

For the collection of the plant endmembers, pixels that were dominated by vegetation were isolated by applying an NDVI-based mask to the image. The threshold for the mask was set to differentiate between dominantly vegetation and non-vegetated landcover, at a value of .40. This value was based on empirical tests of several thresholds on this data set. The threshold effectively excluded large (>> 1 pixel) soil-dominated areas, but retained portions of small roads that were adjacent to vegetated areas that

displayed vegetation signatures resulting from mixing of vegetation with pavement or soil. This effectively included all significant vegetation within the scene in the masked "vegetation-only" image. All 35 coherent MNF bands were input to the n-dimensional visualizer for selection of the plant endmembers (Figure 4B).

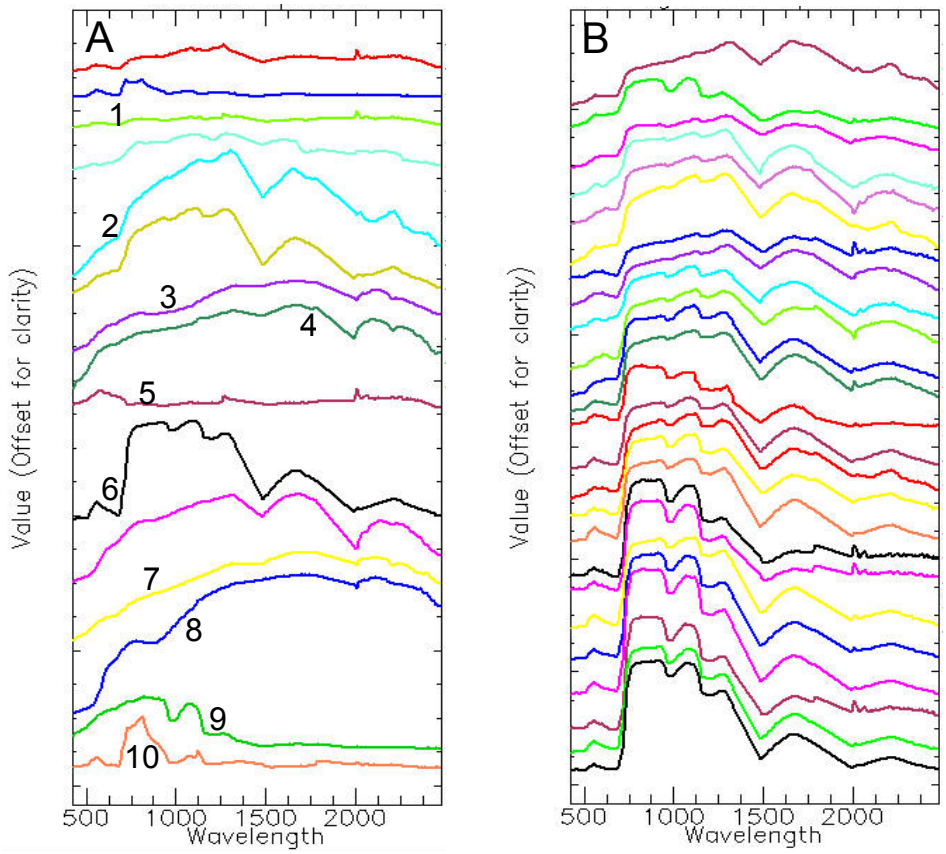

Figure 4. A sample of the general endmember spectra (derived from full image) is shown in A, including examples of shadow (1), senescent vegetation (2), soil and rock classes (3,4,7,8), water (5), vegetation (6), silty water (9), and eutrophic water (10). B includes sample vegetation endmember spectra (derived from the NDVI-masked image).

3.2 Modified strategy for endmember collection

Generally, when endmembers are selected using the n-dimensional visualizer in ENVI, aggregates of pixels are selected at the outer extremes of spectrally well-separated extensions from the central pixel cloud (ENVI, 2003). This strategy was used to select the general landcover endmembers (Figure 5A). Because the pixels from the masked image were dominated by vegetation, however, the pixel cloud was spectrally homogeneous, and presented very few unique, well-defined extensions in spectral space. A different strategy was used, therefore, to select the vegetation endmember set. Only the most extreme few pixels on the ends of small protrusions from the more homogeneous pixel cloud were selected to represent potential species endmembers (Figure 5B). There were many more of these subtle extensions than the number of input MNF bands, however, and any possible unique set of pixels on these extensions was collected. The selection of potential endmembers continued until no additional extreme pixels could reasonably be obtained. Sixty-one potential vegetation endmembers were collected, and it was assumed that a complete set of endmembers had been extracted for this scene. Both the vegetation and general landcover spectra were edited for consistency, redundant classes were removed, the mean spectrum for each class was calculated and then added to the spectral library. The two libraries were combined, with

the final complete libraries containing 62 (for 1999) and 63 (in 2001) total endmembers. All endmembers were input to the MTMF algorithm, however, the classified scenes were dominated by only 20-25 classes, with several classes represented by only a few pixels in all the flightlines.

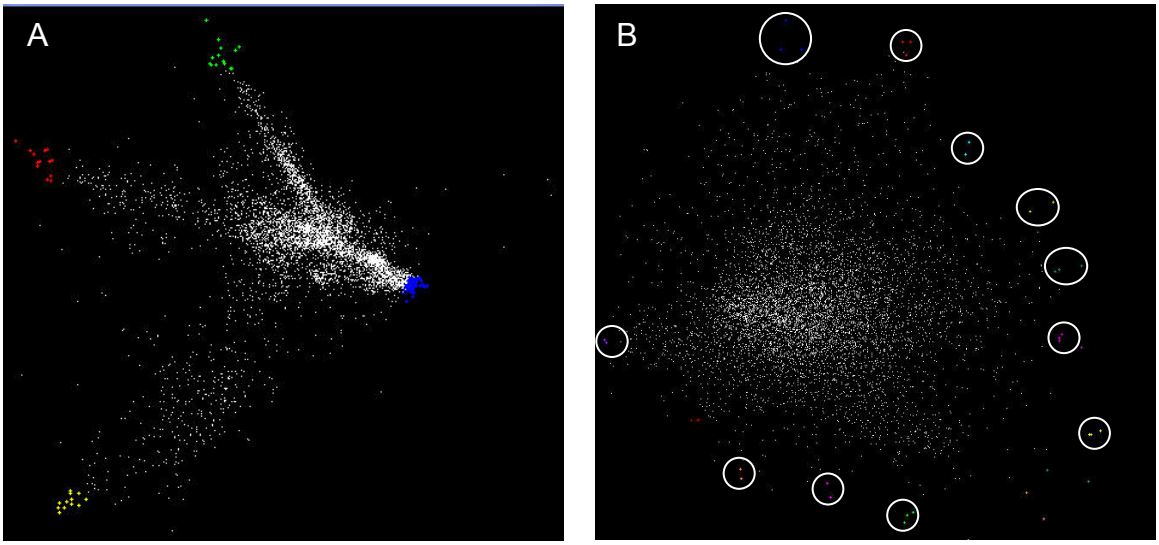

Figure 5. Two-step selection of endmembers from ND-visualizer scatter plots. A: general landcover class selection using large clusters of isolated extreme pixels from full image; B: vegetation endmember selection from small, subtle extensions from the more homogeneous, centralized vegetation cloud, using small groups of pixels (generally 2-5 pixels per class) from masked image.

3.3 Spectral libraries for multiple flightlines: comparisons and retransformations

To map multiple flightlines, two options can be used for the input image-derived spectral library: 1) a single library, derived from one flightline then applied to all other flightlines or 2) individual spectral libraries, derived independently from each flightline, and used to map that respective flightline. To test which approach was more appropriate for multi-flightline, multi-temporal mapping and change detection, test maps were produced using both options. With 35-40% sidelap between flightlines, it was possible to test the consistency of maps from one flightline to the next for the spectral library options by comparing classifications of identical areas from adjacent, overlapping flightlines. Figure 6A indicates the maps of identical areas classified on flightlines 1 and 3 that were produced using two unique libraries (i.e., one library was derived from and used to map flightline 1, and a second from flightline 3). Overall landcover was consistent within the coverage of the two test flightlines; therefore, it was expected that the endmember classes extracted from each of the flightlines would be similar. Roughly equivalent groups of pixels were defined as distinct classes on the two flightlines. It was difficult to directly compare the results, however, because the libraries were not identical and class codes varied. Seamless mosaics could not be produced without recoding and re-coloring equivalent classes between flightlines. With several flightlines and many endmembers, recoding all flightlines to the identical class codes (and colors) would be cumbersome and time consuming.

To avoid coding problems, a single spectral library, derived from flightline 1, was applied directly to map all four flightlines from a single date. The results from flightlines 1 and 3 are shown in B. Because the identical library was used to map both flightlines, the green endmember class should indicate leafy spurge in both images. It is correctly mapped on flightline 1, but incorrectly on flightline 3 (see Figure 6, B1 vs. B3). It is difficult to identify a single spectral class that represents leafy spurge in the classified image from flightline 3. The remaining vegetation classes also do not correspond well between the two flightlines.

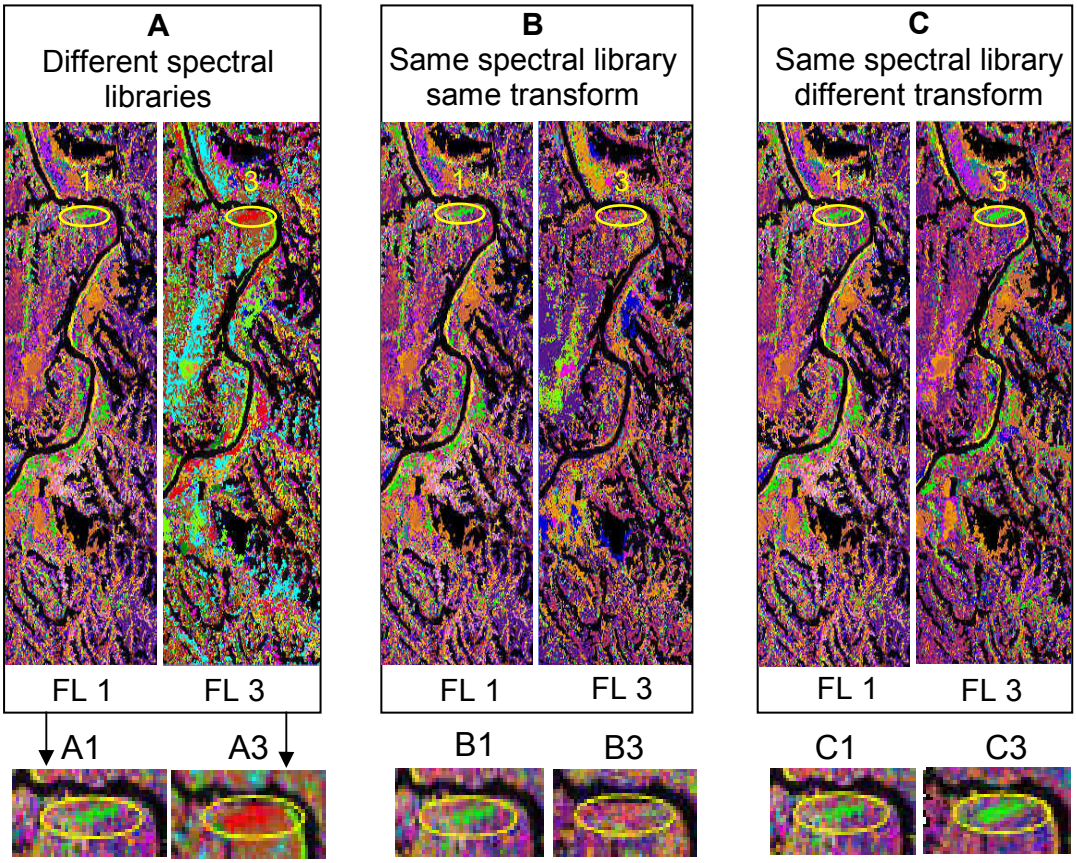

Figure 6. Spectral library effects between flightlines. The area of leafy spurge circled in yellow is enlarged below each corresponding flightline. Green pixels indicate a known leafy spurge patch in A1, B1, and C1 (which are identical classifications). Spurge is well-defined in the corresponding flightline 3 area for A3 and C3, but poorly classified in B3. Comparisons are difficult between A1 and A3 due to mismatched codes between the 2 separate libraries. C (same library, different transformation) provides the most consistent, interpretable results between flightlines.

If the original single spectral library derived from the single flightline is inverse transformed, however, then re-transformed using the MNF statistics files that were generated during the MNF transformation of each individual flightline, and then used to classify that flightline , very good class correspondence is obtained from one flightline to the next (see Figure 6, C1 and C3). Using this single, re-transformed spectral library allows processing to be streamlined by eliminating the need to extract spectral libraries from each flightline, or to adjust codes following classification. Mosaicing and analyses between flightlines are facilitated because the original input spectra are the same, all classes are identical, and coding is consistent from one flightline to the next.

3.4 Modified, hybrid MTMF application

Modifications of the MTMF application focused on reducing interactive decisions during processing, and specifically included altering the input endmembers, as well as developing a new strategy for post-classification thresholding. A hybrid approach used the logic of linear spectral mixture analysis (SMA), while the MTMF algorithm was applied for the actual mapping.

A critical modification involved running the MTMF algorithm with all possible endmembers, using an approach that amounts to a hybrid between linear SMA and MTMF. It is generally considered an advantage of the MTMF that it requires only one to a few target endmembers to map specific materials.

To use this approach, however, the target endmember spectrum must be unequivocally identified prior to mapping. This can be difficult for plant species or assemblages, particularly when a large number of similar endmembers have been extracted from an image. For this reason a hybrid approach was used. All possible endmember classes were input to the algorithm, similar to linear SMA mapping in which all endmembers must be represented in order to simultaneously retrieve the endmember fractions (Adams et al., 1993). With SMA, however, the total number of endmembers is actually restricted to the number of input bands plus 1. Based on homogeneity of spectral plots as well as visual absence of spatial patterns in the imagery, 34-36 MNF bands (depending on flightline) were considered coherent enough to use for mapping in this study. This would mathematically restrict the number of endmembers to 35-37, if the SMA algorithm was used. If there appeared to be additional endmembers, they would not be used for mapping and the target endmember could be excluded. The exhaustive endmember set collected from this data, for example, contained 63 possible endmembers, and if SMA was used, nearly half of these would be discarded. With the modified MTMF, by inputting all endmembers, no *a priori* decision regarding the most appropriate target spectrum was required. Once mapping was completed, however, the target class and endmember spectrum were readily identified by using a GIS overlay of vegetation polygons, including leafy spurge patches, on the classified image. These polygons were delineated by continuously collecting GPS point locations while circumscribing the perimeter of vegetation patches in the field.

The method for selecting MTMF thresholds was modified by automating the process using: 1) a rule classification to establish the MF threshold; and 2) applying a standard +1 sigma for selecting the infeasible threshold. The output of the MTMF algorithm is a matched filter (MF) score image and an infeasibility image for each endmember. In the traditional application of this algorithm, maps are produced from the MTMF results by selecting hard thresholds for the target class(es) from a graphics display of MF score versus infeasibility score (Boardman, 1998). Pixels with high MF and low infeasibility scores represent the most suitable values for accurately defining a class. These are selected manually by defining a region of interest (ROI) around the selected combination of MF and infeasible values. This approach is subjective, however, and thresholds will vary from one analyst to another, one time to another, as well as between flightlines. Even within a single flightline the selection will vary because the graphical method only applies the threshold to those pixels that are within the currently displayed image window. A test of this standard method indicated that minor variations in the ROI produced critical differences in leafy spurge maps (Figure 7). An accurate map could be produced with this method (i.e., Figure 7C), but to do so required several manual adjustments of the ROI until the resulting map corresponded to known occurrences of leafy spurge on the ground.

A different approach was developed to remove subjective boundary decisions on the part of the analyst. Initially a post-classification "rule classifier" (ENVI, 2003) was used to produce a fully classified, thematic map similar to the output from traditional multi-spectral classifiers (Lillesand and Kiefer, 2000). All 63 endmember matched filter images were included in the rule classification, with the assignment of the dominant class based on the highest of the 63 MF scores for each pixel. This allowed a map of the dominant material within each pixel to be produced, without requiring a decision on an absolute, single threshold. With this technique, manual adjustment of thresholds based on intimate knowledge of the ground was not required, and the threshold was automatically determined individually for each pixel rather than forcing the selection of a single image-wide threshold.

A map of the leafy spurge target class was produced from the classified map by masking and isolating pixels that mapped as leafy spurge as the dominant class. This leafy spurge map was then refined using a standardized infeasibility threshold. Based on several test thresholds, +1 sigma above the mean infeasibility score from the target image was selected as the standard. This was determined to be an appropriate boundary for leafy spurge, for all eight flightlines classified in this study; however, this boundary was not tested on other vegetation classes. The +1 sigma value placed the thresholds for each image at a value that eliminated most known false positives, while no large or obvious known patches of leafy spurge were omitted. By applying this as the standard threshold no interpretive decision was required by the analyst to establish the infeasible threshold.

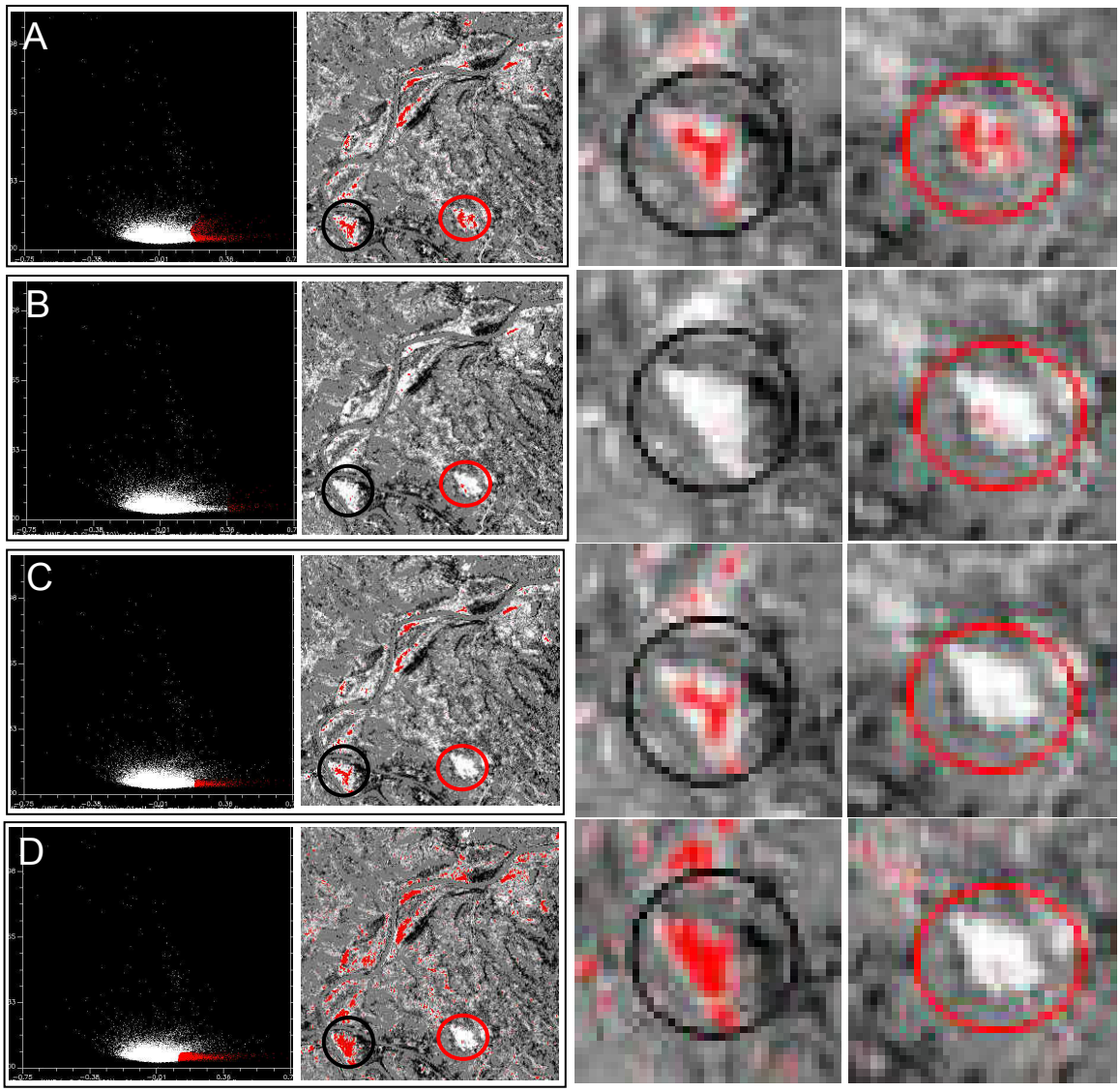

Figure 7. User-defined graphical selection of thresholds. Red pixels are those that have been labeled leafy spurge, based on the corresponding scatter plot ROI to the left. The area circled in black contains a known dense infestation of spurge; the red circled area is known to be free of leafy spurge. In A, C, and D the ROIs have correctly included MF/infeasible values to map the spurge (see black circles); the A and B ROIs have also incorrectly included values within the leafy spurge mapping threshold for other types of vegetation as well and therefore required adjustment (see red circles). C and D are close to the known occurrence of leafy spurge in the field, but D is overclassified (black circle); while C is slightly underclassified (black circle). Ground reference data was required to adjust the ROIs until the map fits the correct distribution.

The maps produced with the hybrid, modified MTMF method successfully defined known patches of leafy spurge, while at the same time spectrally similar vegetation that had been easily confused with leafy spurge using other classification strategies was effectively excluded (see Figure 8B). The black and red circled areas in this figure correspond to those in Figure 7, and show a similar distribution to the map in 7C, the most correct classification obtained by manually and repeatedly adjusting ROI thresholds; however, the automated, modified mapping method produced a qualitatively accurate classification, without requiring decisions, interpretation, or manual adjustments to produce the best fit to known ground

locations. By using standardized, automated thresholds, results will be more comparable temporally, rather than reflect artifacts due to differences in selected thresholds or manual adjustments by image analysts.

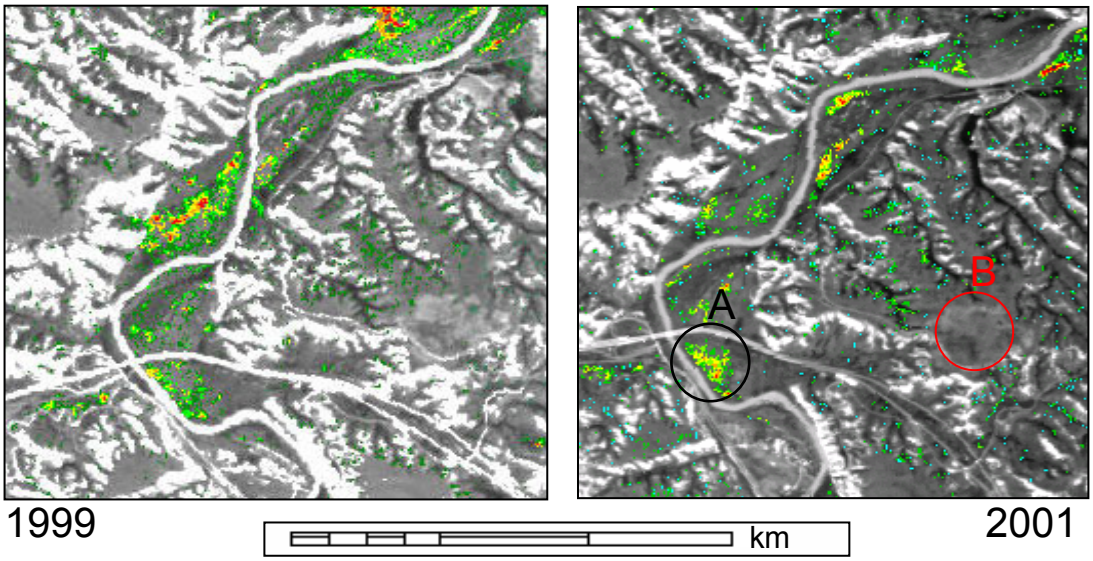

Figure 8. 1999 and 2001 leafy spurge maps produced from modified MTMF. Only pixels in which spurge represents the dominant component are mapped. The relative fraction (abundance?) is indicated by color. Red is highest fraction, followed by orange, yellow, then greens/cyan represent the lowest fraction, leafy spurge classified pixels. On the 2001 map, the black circle labeled A encloses a known area of dense leafy spurge; B (red circle) is an area known to be devoid of spurge.

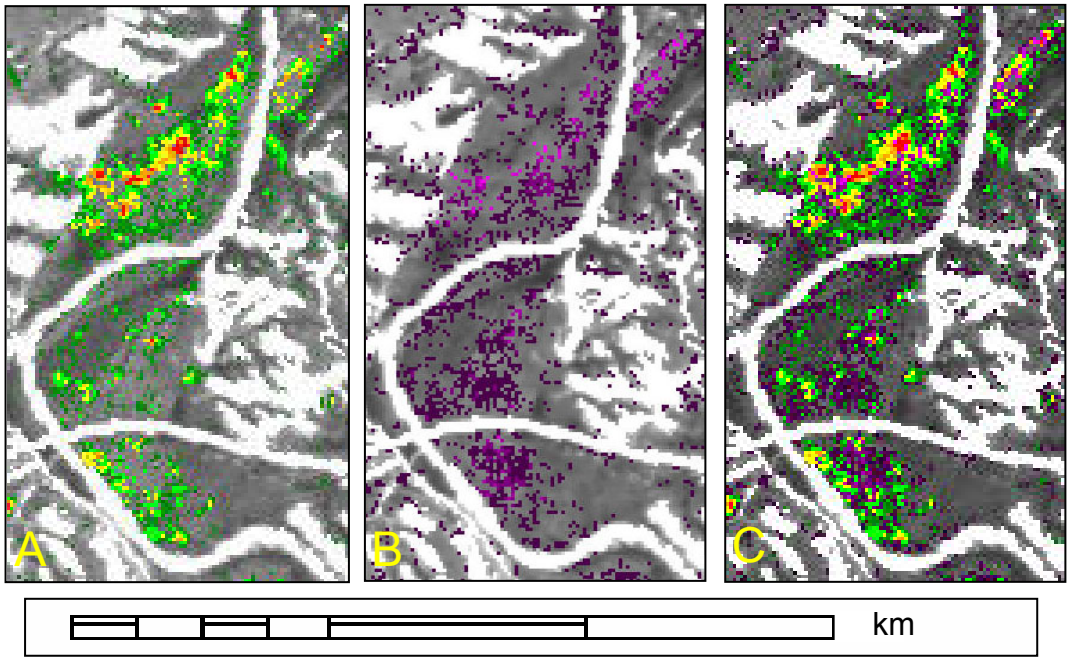

Figure 9. 1999 leafy spurge maps. A: density-sliced categories of primary map (leafy spurge the dominant component of mapped pixels); B: density-sliced map of secondary map (leafy spurge fractions in pixels where weed is a subordinate component); C: primary and secondary density-sliced leafy spurge

maps combined. Lightest magenta: highest fraction; deep magenta lowest; Red: highest fraction, decreasing from orange through yellow, green, and dark green.

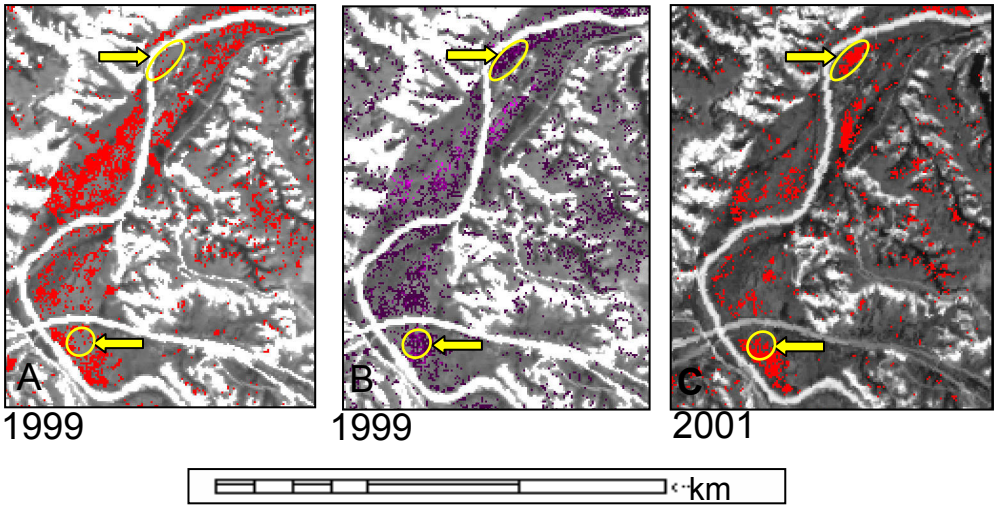

Figure 10. A and C: binary (presence/absence) maps of leafy spurge, 1999 and 2001; B: density sliced map of leafy spurge as subordinate fraction of pixels (lightest magenta represents the highest fraction, deep magenta the lowest fractional abundances).

The final binary leafy spurge maps from 1999 and 2001 were density-sliced, using equal interval MF scores to produce maps that approximate the relative abundance of leafy spurge in those areas where it represented the dominant vegetation within a pixel. The MF score is assumed to represent a surrogate measurement of abundance. The method above yields maps indicating the relative abundance only in pixels in which leafy spurge represents the dominant fraction (Figure 8).

These maps will underestimate the occurrence of leafy spurge, because they do not include the fractional abundance of leafy spurge for pixels in which the weed is a subordinate, yet still significant component of a pixel. To address this problem a secondary leafy spurge map was created using the identical density slice range from the leafy spurge MF image for all pixels that did not map leafy spurge as the dominant class (Figure 9). In Figure 10, areas circled in yellow indicate pixels that did not map as leafy spurge dominant in 1999, but were classified as leafy spurge in 2001. The same areas contain continuous patches of leafy spurge as low fraction, non-dominant components of these same pixels in the 1999 secondary map. Such areas may prove useful as predictors of areas prone to future heavy infestations.

3.5 Rapid, automated vegetation mapping

An intermediate product of the process was a full scene vegetation map for all non-masked pixels (Figure 11, B for 1999 and C for 2001). These maps compared favorably to a published vegetation map (see Figure 11, A) produced from 1:10,000 scale aerial photography (Anderson et al., 1996). The modified MTMF is an alternative to manual photo-interpretation for vegetation mapping, and the maps from 1999 and 2001 compare favorably to the photo-interpreted map, but are more detailed, as it will map the dominant vegetation within 17 m² versus the standard 1- or 5-acre minimum mapping unit used by vegetation mapping programs. This technique also generates significant savings in time and effort for area-wide vegetation mapping.

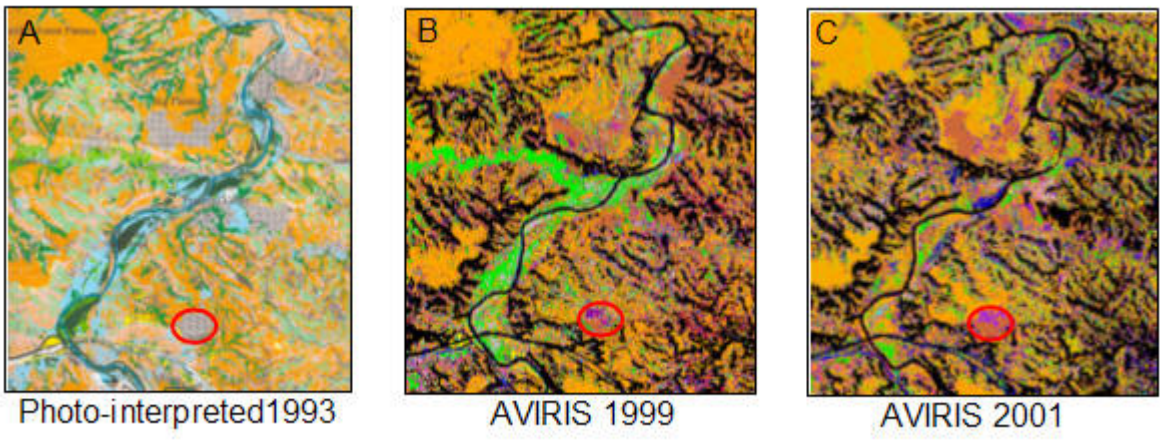

Figure 11. AVIRIS and photo-interpreted maps, showing advance and decline in leafy spurge (light green) between 1993 and 2001. Greater species/assemblage separation seen with AVIRIS maps (i.e., see red circled area that mapped as a single vegetation assemblage on 1993 map, two distinct vegetation classes in 1999 and 2001 AVIRIS maps. Black in the AVIRIS maps indicates non-vegetated landcover that was masked.

4. ACCURACY

Map accuracies were evaluated with a random point-based confusion matrix that is routinely used to validate multi-spectral classifications (Congalton and Green, 1998). Low overall accuracies were indicated: 39% for 1999, and 47% for 2001. User's accuracy values were high, however, (100% in 1999 and 86% in 2001) indicating that relatively little vegetation was erroneously classified as leafy spurge. The low producer's accuracy (26% for 1999 and 18% for 2001), however, suggests that a significant fraction of the leafy spurge was omitted from the map. High omission error was expected, because the accuracy assessments were run on the binary map of leafy spurge as the dominant component of a pixel only. Updated accuracies using the combined leafy spurge dominant and subordinate maps are in progress, however, the type and scale of the validation data (centroids of 3 m x 5 m plots) that were used as reference data in the error matrices was not appropriate for validating 17m data. In addition, because leafy spurge often occurs in small or fragmented patches, the accuracy results were particularly sensitive to registration shifts. Overlay of field-defined vegetation polygons over the raster classifications suggests that the maps are likely better that the error matrices suggest (Figure 12). A visual comparison of the

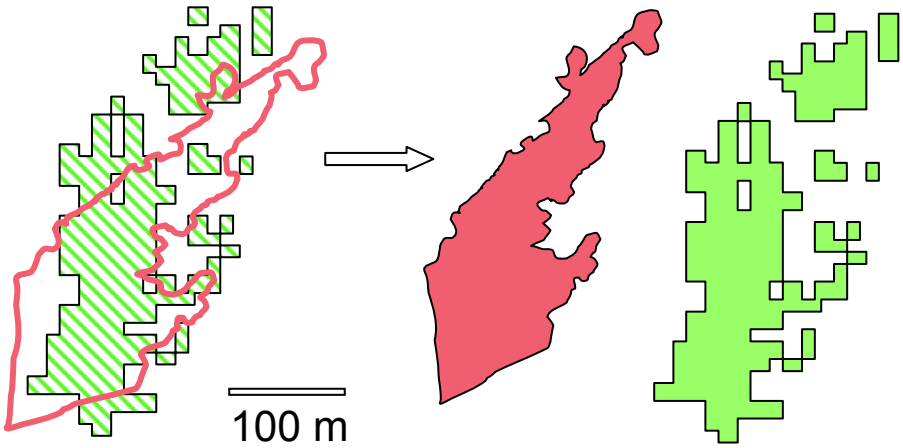

Figure 12. Field polygon (red) versus classified (green); size and shape correspond, location appears rotated between field location and imagery.

polygon delineated in the field to the area classified as leafy spurge suggests that the refined mapping method used here works well, but also suggests that registration problems persist between the image and reference data (that registration between image and reference data is problematic); for example, the overlay suggests a rotation between the raster and vector locations, which would result in lower accuracy values if the polygon were used as ground truth in an error matrix.

5. CHANGE MAPS

In spite of registration issues, the binary maps from 1999 and 2001 were successfully used to produce a map of the regional change in distribution of leafy spurge between these two years (Figure 13). In the western region, where bio-control efforts had been concentrated, the dominant blue indicates success of the treatments and reduction in leafy spurge. In the northeast, spotty red patches suggest expansion of leafy spurge in this region. Based on this information, land managers are planning to focus control efforts in this area that was formerly believed to be un-infested. The circled area in Figure 13 is dominated by areas of either no change or expansion of leafy spurge, and was originally believed to be erroneously classified, as this area was considered un-infested as well. A field check indicated heavy infestation with large continuous dense monocultures of leafy spurge, and the area was subsequently targeted for aerial spraying. The change map indicates approximately a 40% decrease in leafy spurge within THRO and the surrounding grasslands and range over the two-year period. Per-pixel change in fractional abundance could not be accurately determined. More precise registration between multi-temporal images will be required in order to complete temporal, pixel-to-pixel analyses, including a comparative study of the effectiveness of different controls that have been applied.

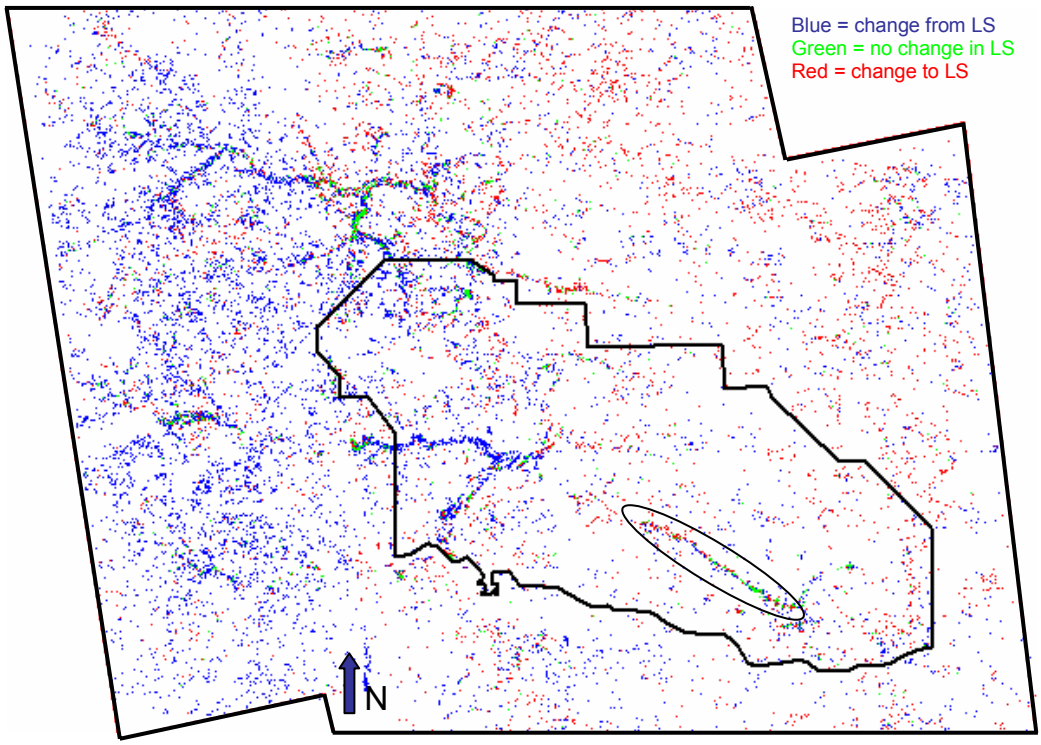

Figure 13. Change in leafy spurge (as the dominant component of a pixel) between 1999 and 2001. Blue indicates leafy spurge in 1999, absent in 2001 (reduction); green indicates leafy spurge both years (no change); red indicates leafy spurge absent in 1999, present in 2001 (expansion).

6. SUMMARY

Initial test maps of leafy spurge varied depending on the method that was used to produce them, indicating that the appropriate methods and algorithms should be selected cautiously. For detailed, accurate mapping of leafy spurge the following steps were critical: a cross-track illumination correction; thorough band editing; and endmembers derived from the image, after NDVI-masking to isolate vegetation. The MTMF algorithm performed well, and the associated infeasibility images allowed the classification to be fine-tuned.

The mapping method was then modified in order to decrease the interactive processing that was required and to increase the consistency of maps, both spatially and temporally. The critical modifications included: 1) separate extraction of general and vegetation libraries from unmasked and masked images, using a 2-step endmember collection with a modified selection strategy used to isolate classes; 2) selecting all possible endmembers from the imagery without restricting the selection to a theoretical maximum number; 3) detailed editing of endmember spectra and the final spectral libraries; 4) MNF retransformation of a single spectral library prior to mapping each flightline; 5) mapping with the MTMF algorithm using a hybrid approach with all possible endmembers as input rather than a single target endmember; 6) using a post-classification rule classifier to establish the MF threshold automatically and eliminate interactive, subjective decisions on MF threshold used for mapping; 7) applying a +1 sigma above the mean score from the infeasibility image to standardize the infeasible threshold selection for refinement of classification.

The modifications outlined above were used to capitalize on the advantages of the MTMF and linear SMA algorithms, while minimizing the drawbacks of each method. The resulting hybrid, modified MTMF method retains the advantages of both methods; for example with MTMF there is no restriction on number of endmembers, it is not necessary to simultaneously solve for all endmembers fractions, and additional infeasibility images are produced that allow maps to be refined. With linear SMA, theoretically all endmembers are derived and fractional abundances of all classes are calculated to produce a fully classified map without requiring decisions on thresholds. The modified method, however, addresses drawbacks of each algorithm and improves specifically on the MTMF application and results.

Because a full suite of all possible endmembers was extracted and used for mapping, and the number of endmembers is not restricted to a theoretical maximum with the MTMF, endmembers for subtly different classes can be collected for allow more successful species mapping. Theoretically, no classes were omitted, therefore a target endmember would not be inadvertently omitted. No *a priori* identification of the specific endmember target was required as is the case with the standard MTMF application using a single endmember. This is advantageous as it can be difficult to select the "most" correct image-derived endmembers before mapping is completed. This also eliminates another interactive decision at this stage of the processing. By using image-derived endmembers, classes are not restricted to those that could be characterized by ground-based spectral measurements.

When all MF scores "compete" for class assignment with the rule classifier, the threshold will automatically adjust as needed on a pixel-by-pixel basis. The best score class from all possible classes is simultaneously assigned, rather than requiring that each target class be individually mapped.

Sub-pixel abundance measurements are retained in the MF score images for each class. The target map can be extracted from the full classification and then coded by fractional abundance, and secondary maps of fractional abundance can also be produced for pixels in which a target is not dominant, but still a significant fraction of a pixel.

In addition to individual maps of specific targets, complete area-wide vegetation maps of the dominant material in each pixel can be produced rapidly and automatically, with greater detail than obtained with standard photo-interpreted vegetation mapping programs. The modified MTMF provides a potentially very useful method for more rapid, automated production of vegetation maps (over the standard manual interpretation of aerial photographs).

Because the spectral library was extracted from a single flightline, but transformed with the appropriate MNF statistics, results are more standardized and comparable between flightlines over a large

area. Spatial and temporal consistency of maps will be improved, and because all class coding is consistent, it allows easier comparisons, mosaicing, and analyses between flightlines.

By eliminating the need to decide on mapping thresholds or target endmembers, the modified MTMF is less interactive, and interpretive input and possible bias by the image analyst is minimized because the thresholds are determined automatically, using standardized criteria and methods. Arbitrary decisions with respect to threshold placement are minimized, and images can be processed with less expertise. Complex technology and processing are more "user friendly", a bonus for monitoring and management applications. By standardizing thresholds, multi-temporal maps will be more comparable, as the thresholds are applied using consistent criteria over time.

Because interactive, manual adjustments are not necessary, the required validation data could potentially be minimized. In addition, the scene-wide threshold variability that results from the graphic threshold selection from isolated blocks of the full image is eliminated. Temporal monitoring is facilitated because results will be more comparable from one date to another. By increasing standardization and consistency of individual maps, change maps produced from them will more accurately represent real landcover changes, rather than apparent change that is actually an artifact of processing differences. By automating, processing is facilitated. A more standardized protocol can be developed, that can be applied more quickly and potentially with less training. Because the processing uses software and algorithms that are commercially available, no unique (in-house) programs or modifications of programs/software were required.

With this modified method, maps were as good as or better than any produced using interactive adjustments, and they were completed more rapidly. By explicitly selecting and defining a procedure, hyperspectral processing will be facilitated, and may lead to increased use by land managers as well as increase the chances of successful temporal and spatial monitoring of leafy spurge and other materials.

Acknowledgements: The authors acknowledge Carol Mladinich of the USGS, RMMC for geo-referencing assistance, Steve Hager at Theodore Roosevelt National Park for logistic, field, lab, GPS, and GIS support, and Diane Larson of the USGS Northern Prairie Science Center for providing field plot data for accuracy assessments. We would especially like to acknowledge our co-author, Ralph Root, a colleague, mentor, and friend- he was instrumental in defining and guiding this study. Sadly, he passed away earlier this year.

7. REFERENCES

Adams, J. B., M. O. Smith, and A. R. Gillespie, 1993, Imaging spectroscopy: Interpretation based on spectral mixture analysis, C.M. Pieters and P.A.J. Englert (Eds.), *Remote geochemical analysis: elemental and mineralogical composition*), New York: Cambridge Univ. Press, pp. 145–166.

Anderson, G.L., J.H. Evert, D.E. Escobar, N.R. Spencer, and R.J. Andrascik,1996, Mapping leafy spurge (*Euphorbia esula*) infestations using aerial photography and geographic information systems, *Geocarto International*, 11:81–89.

Anderson, G.L., E.S. Delfosse, N.R. Spencer, C.W. Prosser and R.D. Richard, 2003, Lessons in developing successful invasive weed control programs, *Journal of Range Management*, 56: 2–12.

Bangsund, D. A., J. R. Baltezore, J. A. Leitch, and F. L. Leistritz, 1993, Economic impact of leafy spurge on wildland in Montana, South Dakota, and Wyoming, *NDSU Agricultural Economics Report No.304*, North Dakota Agricultural Experiment Station, North Dakota State University, Fargo, North Dakota.

Beck, G. K., 1996, Leafy spurge, *Colorado State University Cooperative Extension No. 3*, 107, Natural Resources Series. http://www.colostate.edu/ds/

Boardman, J. W., 1998, Leveraging the high dimensionality of AVIRIS data for improved sub-pixel target unmixing and rejection of false positives: mixture tuned matched filtering, *Summaries of the seventh JPL Airborne Geoscience Workshop,* JPL Publication 97-1, Jet Propulsion Laboratory, Pasadena, California, pp. 55–56.

Callihan, R. H., J. P. McCaffrey, and V. J. Parker-Clark, 1990, Leafy spurge: biology and management. *The Service, December 1990, (Series no. 877)* 5p. Cooperative Extension System, Agricultural Experiment Station, University of Idaho, Moscow, Idaho.

Clark, R. N., A. J. Gallagher, and G. A., Swayze, 1990, Material absorption band depth mapping of imaging spectrometer data using the complete band shape least squares algorithm simultaneously fit to multiple spectral features from multiple materials, *Proceedings of the Third Airborne Visible/Infrared Imaging Spectrometer (AVIRIS) Workshop*, JPL Publication 90-54, Jet Propulsion Laboratory, Pasadena, California, pp. 176–186.

Congalton, R. and K. Green, 1998, *Assessing the Accuracy of Remotely Sensed Data: Principles and Practices,* CRC/Lewis Press, Boca Raton, Florida.

CSES, 2000, *Hyperspectral Imaging and Data Analysis*, Center for the Study of Earth from Space Short Course, June12-16, 2000, University of Colorado, p. 501.

DiPietro, D., S. Ustin, and E. Underwood, 2002, Mapping the invasive plant *Arundo donax* and associated riparian vegetation using AVIRIS, *Proceedings of the 11th JPL Airborne Earth Science Workshop,* Publication 03-4, Jet Propulsion Laboratory, Pasadena, California, pp. 65–74.

Dudek, K. B., 2005, Analysis and refinement of multi-temporal imaging spectroscopy methods for improving monitoring and management of *Euphorbia esula* L. (leafy spurge) in Theodore Roosevelt National Park, Ph.D. dissertation in progress, Colorado State University.

Dunn, P.H., 1979, The distribution of leafy spurge (*Euphorbia esula*) and other weedy *Euphorbia* spp. in the United States, *Weed Science* 27(5):509–515.

Dunn, P.H., 1985, Origins of leafy spurge in North America, *Leafy Spurge, Monograph series of the Weed Science Society of America*, Alan K. Watson, ed., 1985, Chapter 2 (3):7–13.

ENVI User's Guide, 2003, ENVI Version 4.0, September 2003 Edition, Research Systems, Inc.

Galitz, D., 1994, The biology of leafy spurge, *Proceedings: Leafy Spurge Strategic Planning Workshop*, Dickinson, North Dakota, March 29–30, 1994, pp. 57–62.

Geomatica 9 OrthoEngine User Guide, 2003, PCI Geomatics Enterprises, Inc., Richmond Hill, Ontario, Canada, p. 56-57.

Green, A. A., M. Berman, P. Switzer, and M. D. Craig, 1988, A transformation for ordering multispectral data in terms of image quality with implications for noise removal, *IEEE Transactions on Geoscience and Remote Sensing*, 26(1):65–74.

Kennedy, R. E., W. B. Cohen, and G. Takao, 1997, Empirical methods to compensate for a view-angle-dependent brightness gradient in AVIRIS imagery, *Remote Sensing of Environment* 62, 277–291.

Kokaly, R. F., R. Root, and K. Brown, 2001, Mapping the distribution of the invasive species leafy spurge (Euphorbia esula) in Theodore Roosevelt National Park using field measurements of vegetation spectra and CASI imaging spectroscopy data, *Third International Conference on Geospatial Information in Agriculture and Forestry*, Denver, Colorado. 5–7 November, 2001.

Kruse, F. A., A. B. Lefkoff, J. B. Boardman, K. B. Heidebrecht,, A. T. Shapiro, P. J. Barloon, and A. F. H. Goetz, 1993, The Spectral Image Processing System (SIPS) - Interactive Visualization and Analysis of Imaging Spectrometer Data, *Remote Sensing of Environment*, Special issue on AVIRIS, v. 44, pp. 145–163.

Lajeunesse, S., R. Sheley, R. Lym, D. Cooksey, C. Duncan, J. Lacey, N. Rees, and M. Ferrell, 1997, Leafy spurge: biology, ecology, and management, *EB-134, July 1997, Montana State University Extension Service*, 25 p.

Leitch, J. A., L. Leistritz, and D. A. Bangsund, 1994, Economic effect of leafy spurge in the upper Great Plains: Methods, models, and results, *Agricultural Economics Report No. 316*, March 1994. Department of Agricultural Economics, Agricultural Experiment Station, North Dakota State University, Fargo, North Dakota.

Lillesand, T. M. and R. W. Kiefer, 2000, *Remote Sensing and Image Interpretation,* John Wiley & Sons, Inc., New York.

O'Neill, M., S.L. Ustin, S. Hager, R. Root, 2000, Mapping the distribution of leafy spurge at Theodore Roosevelt National Park using AVIRIS, *Proceedings of the 9th Jet Propulsion Laboratory (JPL) Airborne Earth Science Workshop*, JPL Publication 00-18, Jet Propulsion Laboratory, Pasadena, California, pp. 339–347.

Parker-Williams, A. and E. R. Hunt, 2002, Estimation of leafy spurge cover from hyperspectral imagery using mixture tuned matched filtering, *Remote Sensing of Environment* 82, 448–456.

Root, R., S. Ustin, P. Zarco-Tejada, C. Pinilla, R.Kokaly, G. Anderson, K. Brown, K. Dudek, S. Hager, and E. Holroyd, 2002, Comparison of AVIRIS and EO-1 Hyperion for classification and mapping of invasive leafy spurge in Theodore Roosevelt National Park, *Proceedings of the 11th Jet Propulsion Laboratory (JPL) Airborne Earth Science Workshop*, JPL Publication 03-4, Jet Propulsion Laboratory, Pasadena, California, pp. 297–305.

Wallace, N. M., J. A. Leitch, and F. L. Leistritz, 1992, Economic impact of leafy spurge on North Dakota wildland, *NDSU Agricultural Economics Report No. 281*, 23 p. North Dakota Agricultural Experiment Station, North Dakota State University, Fargo, North Dakota.